On the association of Magmatic Microgranular Enclaves (MMEs) and cordierite-bearing monzogranites at the Sierra Bermeja Pluton (SW Spain)

Sobre la asociación de Enclaves Magmáticos Microgranulares (EMM) y monzogranitos con cordierita del plutón de Sierra Bermeja (SO España)

Jon Errandonea-Martin[1], Fernando Sarrionandia[2], Manuel Carracedo-Sánchez[1], Idoia Garate-Olave[1] and José Ignacio Gil Ibarguchi[1]

[1] Dpto. Geología, Facultad de Ciencia y Tecnología, Universidad del País Vasco UPV/EHU, Sarriena s/n, 48940 Leioa (Bizkaia). jon.errandonea@ehu.eus, manuel.carracedo@ehu.eus, idoia.garate@ehu.eus, josei.gil@ehu.eus

[2] Dpto. Geología, Facultad de Farmacia, Universidad del País Vasco UPV/EHU, Paseo de las Universidades, 7, 01006 Vitoria-Gasteiz (Álava). fernando.sarrionandia@ehu.eus

ABSTRACT

Magmatic Microgranular Enclaves (MMEs) included in the cordierite-bearing monzogranites of the Sierra Bermeja Pluton (southern Iberian Massif) have been examined to elucidate their possible petrogenetic linkage. Mineralogical differences such as the absence of Crd and Kfs in the MMEs, or the compositions of Bt and Pl, as well as the lack of correlations of some elements in whole-rock geochemistry, point to a separate origin for the MMEs and host monzogranites. The MMEs could represent minor globules of a more mafic magma injected into and comingled with the host monzogranitic magma, without causing significant modifications in the geochemical characteristics of the latter.

Key-words: *Magmatic Microgranular Enclaves, cordierite-bearing monzogranites, Sierra Bermeja, Central Iberian Zone.*

RESUMEN

Los Enclaves Magmáticos Microgranulares (EMM) del plutón de Sierra Bermeja (Macizo Ibérico meridional) han sido estudiados para esclarecer su posible relación petrogenética con los monzogranitos cordieríticos encajantes. Diferencias mineralógicas como la ausencia de Crd y Kfs en los EMM, o las composiciones de Bt y Pl, así como la falta de correlación de algunos elementos en geoquímica de roca total, apuntan a orígenes independientes para los EMM y los monzogranitos encajantes. Los EMM representarían glóbulos de un magma más máfico inyectado y entremezclado con el magma monzogranítico, sin modificar significativamente las características geoquímicas de este último.

Palabras clave: *Enclaves Magmáticos Microgranulares, monzogranitos con cordierita, Sierra Bermeja, Zona Centro-Ibérica.*

Geogaceta, 69 (2021), 27-30
ISSN (versión impresa): 0213-683X
ISSN (Internet): 2173-6545

Fecha de recepción: 16/06/2020
Fecha de revisión: 23/10/2020
Fecha de aceptación: 27/11/2020

Introduction

Magmatic Microgranular Enclaves (MMEs), frequently also referred to as 'mafic', represent mesoscopic bodies of igneous texture that occur included in granitoids (e.g., Didier and Barbarin, 1991; Barbarin, 2005). They are generally finer in crystal size and more mafic than their host granitoids, and they usually constitute one of the most significant petrogenetic indicators of magma mixing (sensu lato) in plutonic environments (e.g., Castro et al., 1990; Barbarin, 2005). The origin of MMEs has been long-discussed, as it has been the linkage with their host granitoids (Didier and Barbarin, 1991; Barbarin, 2005; Clemens et al., 2017).

Within the Iberian Massif, cordierite-bearing monzogranites have been related petrogenetically in some cases to their MMEs. This led to some controversy as the latter could either represent: (i) an ultimately mantle-derived component that would have interacted subsequently with the host granitic magma (e.g., Castro et al., 1999; García-Moreno and Corretgé, 2000; Alonso Olazabal, 2001; García-Moreno et al., 2006); or, (ii) cogenetic cumulates of early crystallized minerals (e.g., Pascual et al., 2008; Rodríguez and Castro, 2017, 2018).

The zoned Sierra Bermeja Pluton (southern Central Iberian Zone), encompasses several cordierite-bearing monzogranite lithotypes that include minor amounts of coeval mantle-derived dioritoids (vaugnerites; e.g., Errandonea-Martin et al., 2018, 2019). Apparently, these mantle-derived magmas did not affect the geochemistry of host granitoids, which were presumably derived from the melting of different crustal sources (Errandonea-Martin et al., 2019). Considering the contrasting nature of the nearly coeval magma pulses that built the Sierra Bermeja Pluton (Errandonea-Martin et al., 2019), the existence of occasional MMEs in the porphyritic monzogranites that constitute the outer unit of this pluton offers a good opportunity to analyze the association between such MMEs and their host monzogranites.

Petrography

The studied MMEs are rounded to ellipsoidal in shape and up to 50 cm in size. Some of the MMEs include K-feldspar megacrysts derived from the host monzogranites, (± Qz, ± Bt; Fig. 1A, B). These MMEs show a significant lack of chilled margins, and exhibit an igneous microporphyritic texture defined by plagioclase, quartz and biotite microphenocrysts, enclosed in a fine-grained groundmass constituted by the same mineralogy (Pl, Qz and Bt) plus accessory apatite, zircon, monazite and ilmenite (Fig. 1C, D). Modal compositions allow classifying them as biotite tonalites (color index = 18–30).

Plagioclase (up to 2 mm) is euhedral with continuous or oscillatory concentric zoning that leads to well-developed rims (Fig. 1C). Cores usually occur varia-

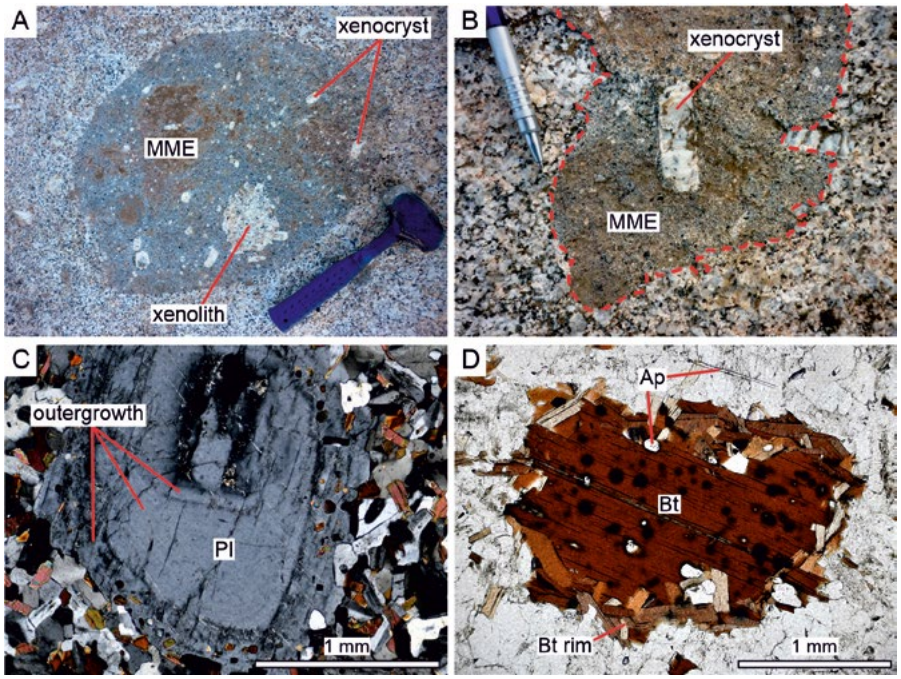

Fig. 1.- A) MME containing xenocrysts of K-feldspar and a xenolith of host monzogranite. B) Detail of a MME enclosing K-feldspar xenocrysts. Note at the right edge of the MME a K-feldspar xenocryst only partially included. C) Optical photomicrograph of a plagioclase (Pl) microphenocryst showing several oriented inclusions and outgrowths. D) Optical photomicrograph of a biotite (Bt) microphenocryst rich in inclusions of quartz and radioactive minerals. This microphenocryst is enclosed by smaller biotite crystals. Note also the acicular habit of the apatite (Ap) of the groundmass. Ver figura en color en la web.

Fig.1.- A) EMM que contiene xenocristales de feldespato potásico y un xenolito de monzogranito encajante. B) Detalle de un EMM englobando xenocristales de feldespato potásico. Obsérvese en el borde derecho del EMM un xenocristal de feldespato potásico sólo parcialmente incluido. C) Microfotografía de un microfenocristal de plagioclasa (Pl) con varias inclusiones orientadas y diversos bordes de recrecimiento. D) Microfotografía de un microfenocristal de biotita (Bt) con abundantes inclusiones de cuarzo y minerales radioactivos. Este microfenocristal está envuelto por cristales menores de biotita. Nótese también el hábito acicular del apatito (Ap) de la matriz. See color figure in the web.

bly altered, although sometimes the intermediate rims appear most altered. It may host numerous inclusions of biotite, often arranged in parallel to the crystallographic faces (Fig. 1C).

Biotite (up to 2 mm) mainly appears as euhedral–subhedral single flakes. Small crystals (< 0.5 mm) constitute an essential component of the EMMs groundmass but they also may occur as polycrystalline aggregates or coating larger biotite microphenocrysts (Fig. 1D). Biotite shows a strong pleochroism and may include apatite, zircon and monazite crystals (Fig. 1D).

It is outstanding the contrasting habit of apatite, from prismatic euhedral crystals present both in the groundmass and as inclusion in biotite microphenocrysts, to markedly acicular ones restricted to the groundmass (Fig. 1D).

Mineral chemistry

Plagioclase shows normal zoning, from slightly altered andesine–oligoclase cores (An_{28}–An_{40}) to fresh oligoclase (An_{18}–An_{28}) rims. These compositions contrast with those of the host monzogranite plagioclase (An_{1}–An_{33}).

Compositional characteristics of biotite also differ from those of the host monzogranites. Biotites of the MMEs display higher mg# (Mg/[Mg+Fe^{2+}]) ratios (up to 0.51) and MgO contents (up to 9.77 wt%) than biotites of the host monzogranites (mg# < 0.45; MgO = 8.27 wt%; Fig. 2). Similarly, TiO_2 and Al_2O_3 contents in biotites from the MMEs (average of 3.48 wt% and 17.89 wt%, respectively) are lower than the host monzogranites biotites (average of 3.65 wt% and 18.47 wt%, respectively). In detail, analyzed microphenocrysts, aggregates and coatings of MMEs biotites have the closest compositions to biotites from the host monzogranites (overlapped area in Fig. 2).

Whole-rock geochemistry

Whole-rock major- and trace-element compositions and Sr–Nd isotopic data of MMEs from the Sierra Bermeja Pluton are given in Tables I and II, respectively. The studied MMEs display lower SiO_2 and K_2O contents than the host monzogranites, showing a calc-alkaline to high-K calc-alkaline affinity (Fig. 3A). They have moderately to highly peraluminous compositions (A/CNK = 1.05–1.23), with Mg# (molar MgO/[FeO^t+MgO]) values in the range of 0.44–0.46, and K_2O/Na_2O ratios between 0.48 and 0.70. They display relatively low CaO (2.33–3.08 wt%) and variable P_2O_5 (0.19–0.40 wt%) contents. They also show higher TiO_2 contents than the host monzogranites (Fig. 3C).

Regarding trace elements, the MMEs display higher Cr, Ni, V, Sc, Zn, Zr, Hf, Nb, Rb, and LREE contents than the host monzogranites, while those of Ba, Pb, Ta and Ga are lower. K/Rb ratios are markedly lower also in the MMEs, whereas La_N/Yb_N values are slightly higher (Fig. 3B).

Isotopic compositions (Sr–Nd) of the selected MME (Table II) were age-corrected to 309 Ma (U–Pb zircon age of the host monzogranites; Errandonea-Martin et al., 2019). The initial $^{87}Sr/^{86}Sr$ ratio of the MME sample (0.7038) is in the range of that of the host monzogranites (0.7028–0.7060) similarly to the εNd_{309} (-2.7) value, which concurs with those of the host monzogranites (-2.6 to -2.7; Errandonea-Martin et al., 2019).

Discussion and conclusions

Several hypotheses have been proposed for the origin of MMEs in general (e.g., Didier and Barbarin, 1991; Barbarin,

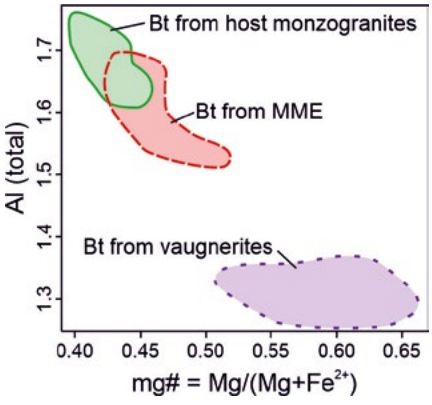

Fig. 2.- mg# vs. Al (total) diagram for biotites from the Sierra Bermeja MMEs, vaugnerites and host monzogranites. Both parameters in a.p.f.u. Ver figura en color en la web.

Fig. 2.- Diagrama mg# vs. Al (total) para las biotitas de los EMM, vaugneritas y granitos encajantes de Sierra Bermeja. Ambos parámetros en a.p.f.u. See color figure in the web.

2005; Rodríguez and Castro, 2018). Accordingly, MMEs may represent: 1) refractory solid residues of partial melting from the source region, 2) xenoliths of wall-rocks, 3) autoliths or cognate fragments of quench cumulates/normal cumulates, or 4) globules of a more mafic magma injected and mingled with the felsic magma. The absence of metamorphic structures and microstructures allows us to discard a restitic origin for the studied MMEs (e.g., Didier and Barbarin, 1991). This, coupled to their compositional characteristics, precludes also their correspondence with wall-rock xenoliths.

An autolithic origin, by rapid and abundant nucleation of near-liquidus minerals caused by thermal quenching, has been proposed for the MMEs from the not far away Los Pedroches Batholith (Donaire et al., 2005). In that case, the studied MMEs would represent cognate fragments of quench cumulates (e.g., Pascual et al., 2008). Experimental data demonstrate that thermal quenching may occur either in the walls of magma chambers or in those of ascent conduits, which would lead to the splitting of an initially homogeneous magma in two compositionally different systems (crystal- and liquid-rich) on account of the crystallization within a thermal-mechanical boundary layer (e.g., Rodríguez and Castro, 2017, 2018). In the case of Sierra Bermeja, mineralogical-geochemical differences between studied MMEs and host monzogranites make difficult an autolithic origin of the MMEs. Whole-rock geochemical data, as the projection in disarray of Sr, Y and HREE, the lower contents in Al_2O_3 and P_2O_5 in MMEs, and the lack of correlations of TiO_2, K_2O, Ni or Rb (controlled mainly by accessory minerals, Bt and Pl), impede a cognate character of the studied MMEs and host monzogranites (e.g., Fig. 3C; Clemens et al., 2017). Moreover, a geochemical modelling performed on the host monzogranites indi-

Sample	MME1	MME2	MME3
	wt%	wt%	wt%
SiO_2	65.26	67.31	65.64
TiO_2	0.71	0.65	0.67
Al_2O_3	17.13	15.28	14.90
$Fe_2O_3^t$	4.59	3.78	4.67
MnO	0.07	0.07	0.08
MgO	1.81	1.59	1.86
CaO	2.89	3.08	2.33
Na_2O	3.79	4.15	3.90
K_2O	2.30	1.99	2.74
P_2O_5	0.19	0.22	0.40
LOI	1.04	0.88	1.54
Total	99.78	99.00	98.73
	ppm	ppm	ppm
Ba	143	178	111
Cr	56.7	14.2	21.4
Cs	24.4	26.1	38.0
Ga	30.7	21.1	19.6
Hf	4.83	5.83	4.44
Nb	14.0	11.5	12.6
Ni	13.6	7.80	11.2
Pb	23.1	16.9	14.5
Rb	364	266	342
Sc	11.0	10.4	11.6
Sn	16.9	12.1	16.3
Sr	144	187	95.9
Ta	1.74	1.45	1.73
Th	16.8	12.3	9.51
U	4.83	3.21	6.32
V	59.8	48.6	60.3
Y	24.4	20.5	22.0
Zn	93.0	62.0	71.1
Zr	190	214	158
La	42.7	42.5	29.4
Ce	84.4	80.1	56.4
Pr	10.2	9.23	6.76
Nd	37.8	27.7	25.8
Sm	6.86	5.20	5.09
Eu	0.934	1.05	0.770
Gd	5.70	4.83	4.41
Tb	0.804	0.660	0.660
Dy	4.16	3.57	3.68
Ho	0.649	0.590	0.600
Er	1.92	1.82	1.81
Tm	0.282	0.280	0.270
Yb	1.74	1.72	1.63
Lu	0.246	0.260	0.230

Table I.- Major- and trace-element whole-rock analyses of the studied MMEs.
Tabla I.- Análisis de elementos mayores y traza de roca total de los EMM estudiados.

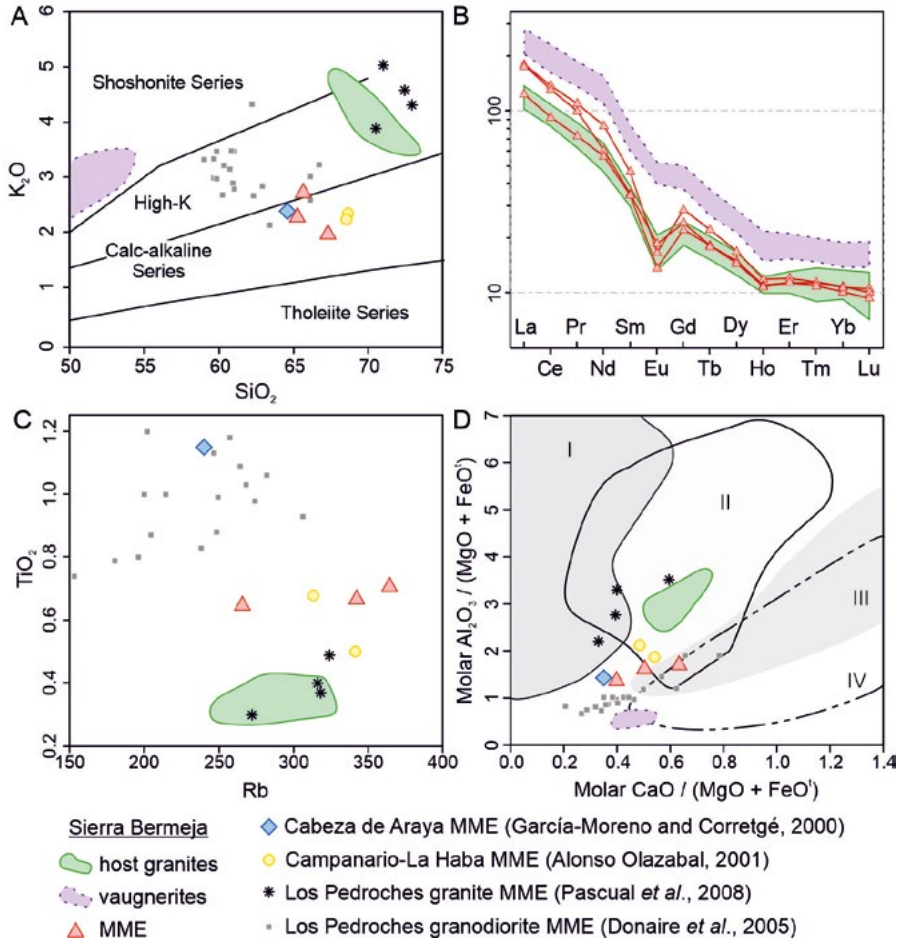

Fig. 3.- A) SiO_2 vs. K_2O diagram of Peccerillo and Taylor (1976). B) Chondrite-normalized (McDonough and Sun, 1995) REE diagrams for the MMEs, host monzogranites and vaugnerites from the Sierra Bermeja Pluton. C) Rb vs. TiO_2 diagram. D) Molar CaO/(MgO+FeOt) vs. Al_2O_3/(MgO+FeOt) diagram based on Gerdes et al. (2002). Partial melts from I: metapelitic sources, II: metagreywackes, III: metatonalites, and IV: metabasalts. Ver figura en color en la web.
Fig.3.- A) Diagrama SiO_2 vs. K_2O de Peccerillo y Taylor (1976). B) Diagramas de REE normalizados respecto al condrito (McDonough y Sun, 1995) para los EMM, los monzogranitos encajantes y vaugneritas del plutón de Sierra Bermeja. C) Diagrama Rb vs. TiO_2. D) Diagrama CaO/(MgO+FeOt) vs. Al_2O_3/(MgO+FeOt), ambos en proporciones molares, basado en Gerdes et al. (2002). Fundidos parciales a partir de I: fuentes metapelíticas, II: metagrauvacas, III: metatonalitas, y IV: metabasaltos. See color figure in the web.

cates that K-feldspar would be a major component of the fractionating mineral assemblage (Errandonea-Martin et al., 2019). Thus, early K-feldspar would be expected in the MMEs as component of the crystal mush, but in contrast, the scarce K-feldspar found in the MMEs shows evidences of being xenocrysts from the host granitic magma (e.g., Fig 1A, B). This fact, together with the absence of coarse-grained textures in the MMEs, excludes also the possibility of the MMEs being normal cumulates from the host granitic magmas. Considering that, we suggest that the studied MMEs and host monzogranites would have separate origins.

Textural characteristics indicate that MMEs were still partially liquid when injected into the host granitic magma (e.g., Kfs and Qz crystals entrained from the host monzogranites; Didier and Barbarin, 1991). Mingling of small volumes of a hot mafic melt with a cooler granitic magma would cause a quench environment that would explain the crystallization of acicular apatite, coating of biotites and complex zoning in plagioclase (e.g., Castro et al., 1990; Clemens et al., 2017). Their small volume and large viscosity contrast with the host granitic magma prevented large-scale mixing (e.g., Didier and Barbarin, 1991), and no pervasive major- and trace-element compositional changes were produced in the MMEs through the mixing (sensu lato) process. Correspondingly, the injection and mingling of the mafic magma did not affect the chemistry of host monzogranites. Instead, the matching between Sr–Nd isotope compositions of the selected MME and host granitoids calls for the decoupling of isotope and element chemical diffusion during mixing (e.g., Pin et al., 1990; Barbarin, 2005). Likewise, no geochemical similarities or apparent trends have been observed towards the compositions of mantle-derived vaugneritic rocks of Sierra Bermeja (e.g., Fig. 3). Moreover, unlike the MMEs, vaugneritic magmas intruded after the emplacement of the later inner unit (Errandonea-Martin et al., 2018), thus making difficult a potential relationship.

While further analyses would be required to establish accurately the source of the studied MMEs, two likely scenarios are suggested: 1) melting of crustal metaigneous sources (e.g., Fig. 3D), similar to those proposed by Donaire et al. (2005) and Pascual et al. (2008), and 2) hybridization of mantle-derived magmas (different to those of the vaugnerites) by assimilation/mixing processes with crustal rocks prior to their injection into the monzogranitic magmas (e.g., Castro et al., 1990, 1999; García-Moreno and Corretgé, 2000; García-Moreno et al., 2006). What seems most certain is that the studied MMEs were injected during a relatively late magmatic stage, without causing significant effects in the nature of the host monzogranites.

Isotope ratio	MME2	2σ error (abs)
$^{87}Rb/^{86}Sr$	4.123	
$^{87}Sr/^{86}Sr$	0.721888	8E-06
$^{87}Sr/^{86}Sr_{309}$	0.7038	
$^{147}Sm/^{144}Nd$	0.1132	
$^{143}Nd/^{144}Nd$	0.512332	6E-06
$^{143}Nd/^{144}Nd_{309}$	0.512103	
εNd_{309}	-2.7	

Table II.- Whole-rock Sr-Nd isotopic compositions of the selected MME (measured and age-corrected to 309 Ma).
Tabla II.- Composiciones isotópicas de Sr-Nd de roca total del EMM seleccionado (medidas y recalculadas a 309 Ma).

Acknowledgements

This work was financially supported by the project CGL2015-63530-P (MINECO/FEDER, EU). I. Garate-Olave was funded by the UPV/EHU grant ES-PDOC19/111. Finally, the authors would like to thank Antonio Castro and Carlos Villaseca for their useful comments, as well as Aitor Cambeses for the editorial handling.

References

Alonso Olazabal, A. (2001). *El plutón de Campanario-La Haba: caracterización petrológica y fábrica magnética*. PhD. Thesis, Univ. del País Vasco, 323p.

Barbarin, B. (2005). *Lithos* 80, 155-177.

Castro, A., Moreno-Ventas, I. and de la Rosa, J.D. (1990). *Geological Journal* 25, 391-404.

Castro, A., Patiño Douce, A.E., Corretgé, L.G., de la Rosa, J.D., El-Biad, M. and El-Hmidi, H. (1999). *Contributions to Mineralogy and Petrology* 135, 255-276.

Clemens, J.D., Elburg, M.A. and Harris, C. (2017). *Contributions to Mineralogy and Petrology* 172, 88.

Didier, J. and Barbarin, B. (1991). *Enclaves and Granite Petrology*. Elsevier, Amsterdam, 625p.

Donaire, T., Pascual, E., Pin, C. and Duthou, J.-L. (2005). *Contributions to Mineralogy and Petrology* 149, 247-265.

Errandonea-Martin, J., Sarrionandia, F., Carracedo-Sánchez, M., Gil Ibarguchi, J.I. and Eguíluz, L. (2018). *Geologica Acta* 16, 237-255.

Errandonea-Martin, J., Sarrionandia, F., Janoušek, V., Carracedo-Sánchez, M. and Gil Ibarguchi, J.I. (2019). *Lithos* 342-343, 440-462.

García-Moreno, O. and Corretgé, L.G. (2000). *Geogaceta* 27, 67-70.

García-Moreno, O., Castro, A., Corretgé, L.G. and El-Hmidi, H. (2006). *Lithos* 89, 245-258.

Gerdes, A., Montero, P., Bea, F., Fershater, G., Borodina, N., Osipova, T. and Shardakova, G. (2002). *International Journal of Earth Sciences* 91, 3-19.

McDonough, W.F. and Sun, S.-s. (1995). *Chemical Geology* 120, 223-253.

Pascual, E., Donaire, T. and Pin, C. (2008). *Geochemical Journal* 42, 177-198.

Peccerillo, A. and Taylor, S.R. (1976). *Contributions to Mineralogy and Petrology* 58, 63-81.

Pin, C., Binon, M., Belin, J.M., Barbarin, B. and Clemens, J.D. (1990). *Journal of Geophysical Research* 95, 17821-17828.

Rodríguez, C. and Castro, A. (2017). *Lithos* 272-273, 261-277.

Rodríguez, C. and Castro, A. (2018). *Geological Society of America Bulletin* 131, 635-660.